GOSPODARKA SUROWCAMI MINERALNYMI

Tom 25 2009 Zeszyt 3

ANNA PIĘTA*, TOMASZ DANEK*, ANDRZEJ LEŚNIAK**

Numerical modeling of ground vibration caused by underground tremors in the LGOM mining area

Introduction

Undesired effects of mining exploitation include seismic tremors that often cause structures and facilities damages at the ground surface. Seismic energy of the tremor, a distance to the hypocenter and the geological structure of the overburden significantly affect the magnitude of seismic events at the surface. The exact evaluation of the influence of those factors on the amplitude of vibrations is of great importance to the Legnicko-Glogowski Copper District (LGOM), Poland's mining region with underground exploitation where high induced seismicity is observed. Full waveform modeling can be used to identify factors that have the greatest effects on parameters describing ground vibrations.

Elastic field full waveform modeling is nowadays very useful tool of seismology and seismic investigations (Danek, Franczyk 2004). It can be employed at any stage of seismic survey from fieldwork designing through data processing to geological interpretation. The basic advantage of such modeling is that it can reproduce all types of waves generated in media with desired structure complexity. It is also possible to determine velocity components at any point of a modeled geological medium, both at the surface and under the surface (Danek et al. 2008; Pięta et al. 2009).

A lot of popular approaches for estimation of ground surface vibrations caused by seismic tremors are based on statistical models. The accuracy of so estimated velocity is restricted by the method nature itself since it is difficult to enter information on rock medium geology and source mechanism. The method proposed in this paper has no such restrictions.

* Dr inż., ** Prof AFG, dr hab. inż., AGH University of Science and Technology, Faculty of Geology, Geophysics and Environmental Protection, Cracow.

1. Methodology of determination of ground vibration from numerical modeling

1.1. Equation of motion in isotropic medium

The equation of motion for two-dimensional isotropic medium can be written in the Cartesian co-ordinate system as a set of first order hyperbolic equations (Virieux 1986):

$$\begin{aligned}
\rho \frac{\partial v_x}{\partial t} &= \frac{1}{\rho}\left(\frac{\partial \tau_{xx}}{\partial x} + \frac{\partial \tau_{xz}}{\partial z} \right) \\
\rho \frac{\partial v_z}{\partial t} &= \frac{1}{\rho}\left(\frac{\partial \tau_{xz}}{\partial x} + \frac{\partial \tau_{zz}}{\partial z} \right) \\
\frac{\partial \tau_{xx}}{\partial t} &= (\lambda + 2\mu)\frac{\partial v_x}{\partial x} + \lambda \frac{\partial v_z}{\partial z} \\
\frac{\partial \tau_{zz}}{\partial t} &= (\lambda + 2\mu)\frac{\partial v_z}{\partial z} + \lambda \frac{\partial v_x}{\partial x} \\
\frac{\partial \tau_{xz}}{\partial t} &= \mu\left(\frac{\partial v_x}{\partial z} + \frac{\partial v_z}{\partial x} \right)
\end{aligned} \tag{1.1}$$

where:

- (v_x, v_z) – are components of velocity vector,
- $(\tau_{xx}, \tau_{zz}, \tau_{xz})$ – are components of stress tensor,
- $\rho(x, z)$ – is density,
- $\mu(x, z)$ and $\lambda(x, z)$ – are Lame constants.

After applying the staggered-grid finite-difference method for space and time shown in Fig. 1.1, equation (1.1) takes the form (1.2):

$$\begin{aligned}
U_{i,j}^{k+1/2} &= U_{i,j}^{k-1/2} + \frac{\Delta t}{\rho_{i,j}\Delta x}(\Sigma_{i+1/2,j}^{k} - \Sigma_{i-1/2,j}^{k}) + \frac{\Delta t}{\rho_{i,j}\Delta z}(\Xi_{i,j+1/2}^{k} - \Xi_{i,j-1/2}^{k}) \\
V_{i+1/2,j+1/2}^{k+1/2} &= V_{i+1/2,j+1/2}^{k-1/2} + \frac{\Delta t}{\rho_{i+1/2,j+1/2}\Delta x}(\Xi_{i+1,j+1/2}^{k} - \Xi_{i,j+1/2}^{k}) + \frac{\Delta t}{\rho_{i+1/2,j+1/2}\Delta z}(T_{i+1/2,j+1}^{k} - T_{i+1/2,j}^{k}) \\
\Sigma_{i+1/2,j}^{k+1} &= \Sigma_{i+1/2,j}^{k} + (L+2M)_{i+1/2,j}\frac{\Delta t}{\Delta x}(U_{i+1,j}^{k+1/2} - U_{i,j}^{k+1/2}) + L_{i+1/2,j}\frac{\Delta t}{\Delta z}(V_{i,j+1}^{k+1/2} - V_{i,j}^{k+1/2}) \\
T_{i+1/2,j}^{k+1} &= T_{i+1/2,j}^{k} + (L+2M)_{i+1/2,j}\frac{\Delta t}{\Delta z}(V_{i,j+1}^{k+1/2} - V_{i,j}^{k+1/2}) + L_{i+1/2,j}\frac{\Delta t}{\Delta x}(U_{i+1,j}^{k+1/2} - U_{i,j}^{k+1/2}) \\
\Xi_{i,j+1/2}^{k+1} &= \Xi_{i,j+1/2}^{k} + M_{i,j+1/2}\frac{\Delta t}{\Delta z}(U_{i,j+1}^{k+1/2} - U_{i,j}^{k+1/2}) + M_{i,j+1/2}\frac{\Delta t}{\Delta x}(V_{i+1,j}^{k+1/2} - V_{i,j}^{k+1/2})
\end{aligned} \tag{1.2}$$

where:

- k – is time step index,
- i, j – are co-ordinates of point in which values of velocity vector and stress tensor are calculated,

Δt – is time step,
Δx and Δz – are distances between computational nodes in x and y direction, respectively,
(U, V) – are components of velocity vector,
(Σ, Ξ, T) – are components of stress tensor.

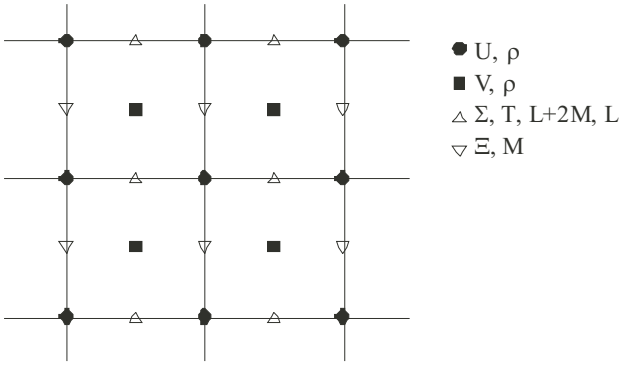

Fig. 1.1. Staggered grid scheme. Black symbols are for velocity components and density at time $(k+1/2) \cdot \Delta t$. White symbols are for stress components and Lame coefficients at time $k\Delta t$

Rys. 1.1. Schemat siatki o węzłach wzajemnie przesuniętych. Zaczernione pola odpowiadają węzłom, w których obliczane są składowe wektora prędkości i gęstość dla czasu $(k+1/2) \cdot \Delta t$. Symbolami niezaczernionymi zaznaczono węzły, gdzie obliczane są składowe tensora naprężeń oraz współczynniki Lamego dla czasu $k\Delta t$

Velocity vector components $(U, V) = (v_x, v_z)$ for time $(k+1/2)\Delta t$ and stress tensor components $(\Sigma, \Xi, T) = (\tau_{xx}, \tau_{zz}, \tau_{xz})$ for time step $(k+1)\Delta t$ are calculated using velocity vector components calculated for time $(k-1/2)\Delta t$ and stress tensor for time $k+\Delta t$. Coefficients L and M correspond to Lame constants λ and μ, respectively.

The stability condition for solution (1.2) can be presented as

$$V_p \Delta t \sqrt{\frac{1}{\Delta x^2} + \frac{1}{\Delta z^2}} < 1 \tag{1.3}$$

where:
V_p – is P-wave velocity.

1.2. Geological model

Seismic wave propagation was modeled for the LGOM mining area. Figure 1.2 presents two generalized geological models characteristic for the study area: a monocline, and a monocline cuted by a number of thrust faults (after Oberc and Serkies 1970).

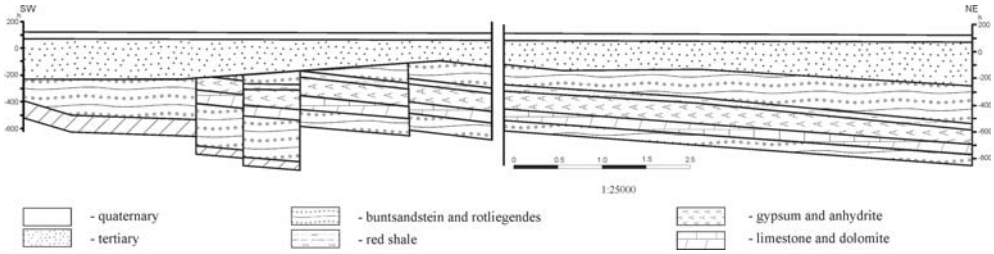

Fig. 1.2. Geological model of study area

Rys. 1.2. Model geologiczny obszaru badawczego

Seismic wave velocities assumed for layers of either model are given in Table 1.1. Values for *P*-wave velocity were taken from logging data for LGOM. *S*-wave velocities were calculated based on laboratory measurements of rock rigidity (Plewa 1977) and geophysical data from surveys made by the Geophysics Department of Faculty of Geology Geophysics and Environmental Protection, AGH UST.

TABLE 1.1

Velocity of seismic waves in geological layers

TABELA 1.1

Prędkości fal sejsmicznych typu *P* w poszczególnych warstwach modelu

Lithology	P-wave velocity [m/s]
Quaternary	1100
Tertiary	1500
Buntsandstein, rotliegendes	2000, 4500
Red shale	2600
Gypsum, anhydrite	2700
Limestone, dolomite	3300
Crystallinicum	6000

1.3. Study methodology

Modeling of seismic wave propagation was made for models of 5750 m length and 1500 depth (monoclinal model) and 6100 m length and 1200 m depth (monocline cuted by thrust faults). The calculation grid nodes were 1 m apart.

Seismic tremor was approximated with a Ricker signal with unit amplitude and 20 Hz frequency; therefore the obtained results of vibrations amplitudes are not absolute. A tremors were generated at selected points of the model, which corresponded to the locations of the assumed quake sources. Due to restrictions imposed by the stability condition described by equation (1.3) and time-shift of the applied calculation grid, it was necessary to

implement 15 000 calculation steps over 1 s time window. Components of the velocity vector and stress tensor were calculated at each point of the calculation grid. Only maximum values of velocity calculated for points that corresponded to sites at the ground surface were chosen to the analysis. A stable source mechanism of double couple force and constant tremor energy normalized to unit were assumed. The shear mechanism was modeled as a set of two mutually perpendicular force dipoles, each of which was modeled as a set of two opposite forces.

To study the influence of the analysed factors on the ground vibration velocity, the modeling was repeated for a variety of ranges of starting parameters, while the attenuation was not allowed for. The analysed factors included changes of the position of seismic tremor hypocenter, change of nodal plane inclination, and different inhomogeneity degree of the near-surface layer.

2. Modeling results

Seismic wave propagation was modeled for earthquake sources located in a dolomite layer, in which a vast majority of tremors recorded in the LGOM mining area are induced by mining activity. Further in this section, we present the analysis of key geological and seismic source factors affecting maximum ground vibration velocity. In next three sections we compare geological models with a homogeneous and inhomogeneous subsurface layer. The inhomogeneity was added through a random disturbance of velocity in the subsurface layer that reached 10% of its initial value.

2.1. Dependence of maximum ground vibration velocity on tremor source location

First, we analysed the dependence of ground vibration velocity and tremor source position. The tremor sources were located in the dolomite layer, both for a monoclinal and a faulted medium. The change of location was connected with NE dip of geological layers, including limestone and dolomite layers. A relationship between ground vibration velocity and different source locations is shown in Fig. 2.1. Additionally, location of tremor sources are marked and numbered in the figure. Velocity values shown in Fig. 2.1 were obtained by averaging maximal vibration velocities for a single seismic tremor. The calculations were made for a geological model containing a homogeneous subsurface layer (solid black line) and a model with random distribution of inhomogeneities in the subsurface layer (dots). The calculated vibration velocity values were typically higher by $5.5 \cdot 10^{-7}$ for a monoclinal model with no inhomogeneity in the subsurface layer, while they were higher by some $7.2 \cdot 10^{-6}$ m/s for a faulted model with no inhomogeneity.

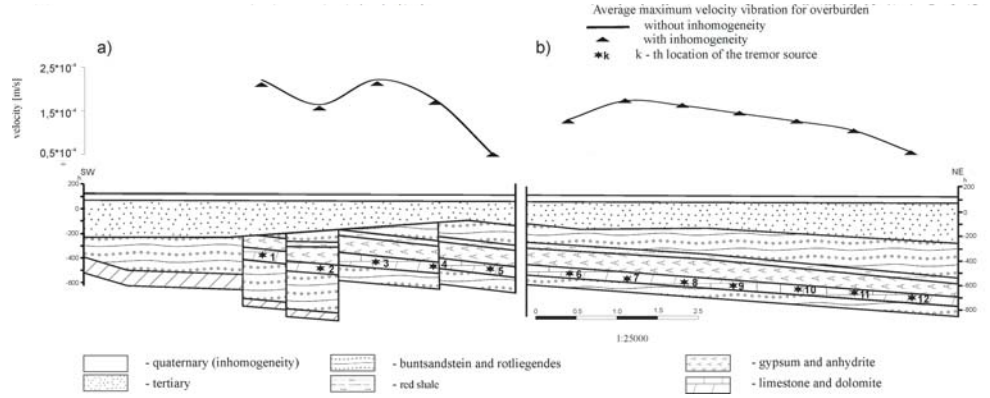

Fig. 2.1. Relation between average maximum velocity vibration and source location for (a) faulted and (b) monoclinal model

Rys. 2.1. Zależność uśrednionych maksymalnych prędkości drgań gruntu od położenia źródła wstrząsu dla modelu zuskokowanego (a) i monoklinalnego (b)

2.2. Effects of tremor source depth on velocity

Next, effects of inhomogeneities on the distribution of maximal ground vibration velocities recorded at the ground surface was analysed. Figure 2.2 shows plots of maximum velocities obtained for a changed location of the source in site 2 (see Fig. 2.1).

Figure 2.3 shows plots of maximum velocities obtained for a changed depth of the tremor source in the monoclinal area (source location No 9 in Fig. 2.1).

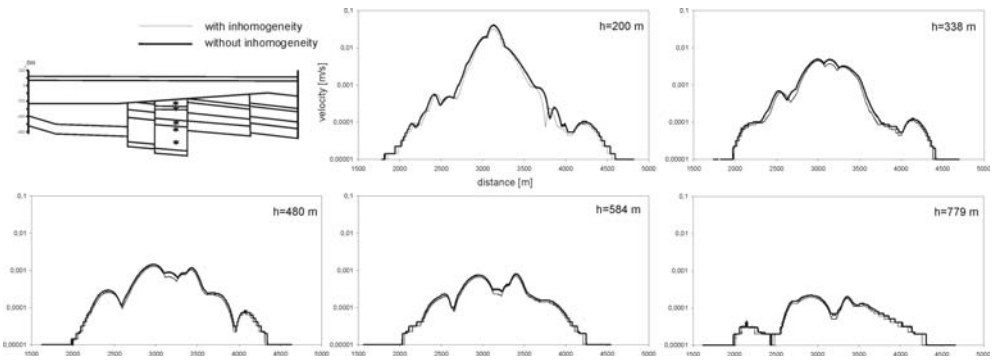

Fig. 2.2. Relation between amplitudes of vibrations and depth of tremor source for monoclinal area with faults

Rys. 2.2. Wykres zmian maksymalnych prędkości drgań terenu dla różnych głębokości źródła wstrząsu dla obszaru monokliny z serią uskoków zrzutowych

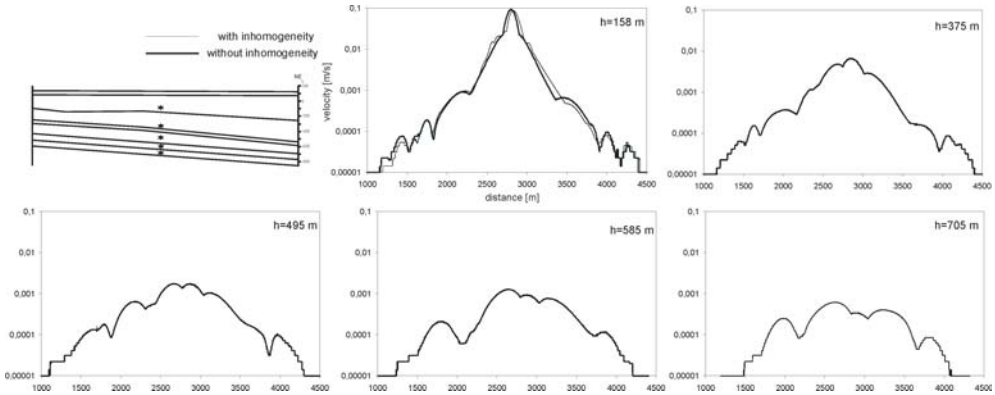

Fig. 2.3. Relation between amplitudes of vibrations and depth of tremor source for monoclinal area

Rys. 2.3. Wykres zmian maksymalnych prędkości drgań terenu dla różnych głębokości źródła wstrząsu dla obszaru monokliny

Increased values of ground vibration velocity recorded at the surface were observed for a geological model with no inhomogeneity in the subsurface layer, both for a monocline model and a thrust faulted model. In either case, changing a depth to the seismic source allowed a zone of high ground vibration velocity to be located. In that zone a significant correlation between change of ground vibration velocity and change of tremor hypocenter was observed. For a model with faults, that zone occurs at a distance of 700 m from the hypocenter (from 2400 m to 3800 m for model in Fig. 2.2) while for a monoclinal model – 500 m form the hypocenter (from 2300 m to 3300 m in Fig. 2.3).

2.3. Influence of source mechanism on vibration velocity values

We analysed also the effects of changing the inclination of planes of strike-slip fault that was assumed as a mining tremor source. Figure 2.4 shows the dependence of maximum vibration velocities recorded at the surface for sources whose fault planes were inclined at the angle of –30°, –15°, 0°, 15°, 30° to the ground surface. Recording was carried out for a monoclinal model with the source at location No 9 at a depth of h = 158 m. A minor effect of inclination angle of nodal planes on values of maximum velocities recorded at the ground surface was observed both for a model with fault and a monoclinal model. Plots of maximum velocity calculated for a monoclinal model show odd parity features. Having normalized plots of maximum ground vibration velocity to velocity plots calculated for the nodal plane with inclination angle of $\delta = 0°$ we observed that maximum velocity plots for nodal planes with the same angle δ but different sign, are symmetric against the straight line that is perpendicular to the ground surface and passes through the seismic hypocenter (Fig. 2.4).

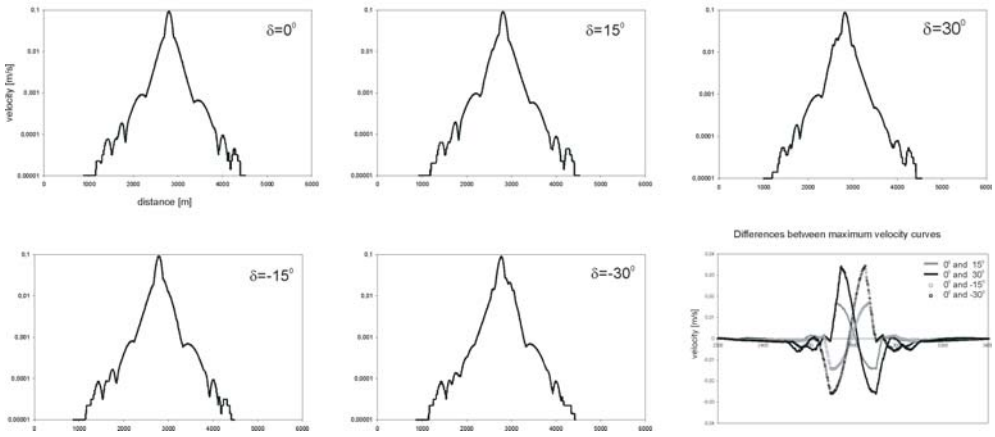

Fig. 2.4. Relation between amplitudes of vibrations and orientations of nodal planes of seismic source

Rys. 2.4. Wykres zmian maksymalnych prędkości drgań terenu dla różnych orientacji płaszczyzn modalnych

2.4. Effect of inhomogeneity degree on vibration velocity

Finally, we analysed the influence of inhomogeneity degree of the subsurface layer on maximum values of ground vibration velocity. Figure 2.5 shows differences between averaged maximum ground vibration velocities obtained from numerical modeling for different inhomogeneity degree (1%, 2.5%, 5% and 10%) of the subsurface layer. The inhomogeneity degree of e.g. 10% was obtained by applying variations (up to 10%) of the initial value of seismic wave propagation velocity in the subsurface layer. A relationship between averaged maximum velocities recorded for a geological model with different inhomogeneity degree of the subsurface layer is shown in Fig. 2.5. Table 2.1 contains averages of maximum velocities

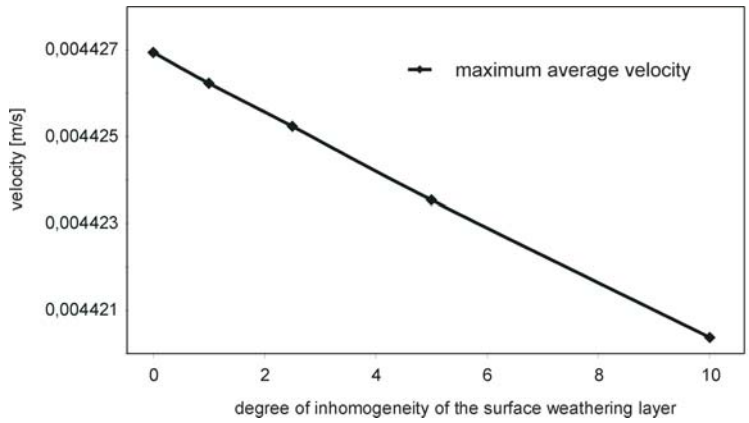

Fig. 2.5. Relation between amplitudes of vibrations and inhomogeneities in surface weathering layer

Rys. 2.5. Zależność pomiędzy uśrednionymi maksymalnymi wartościami prędkości drgań terenu i stopniem niejednorodności warstwy przypowierzchniowej

TABLE 2.1

Average maximum velocity values for models with various inhomogeneity degree of surface weathering layer

TABELA 2.1

Uśrednione maksymalne wartości prędkości drgań powierzchni terenu dla modeli o różnym stopniu niejednorodności warstwy przypowierzchniowej

Onhomogeneity degree	Averaged normalized maximum velocity of ground vibration [m/s]
0% (no inhomogeneity)	0,00442694
1%	0,00442623
2,5%	0,00442523
5%	0,00442354
10%	0,00442037

obtained from numerical modeling for a maximum velocity in the source of 10 m/s. Since the energy attenuation was neglected in the modeling, the obtained results can be easily re-calculated for any velocity assumed in the tremor source.

Inhomogeneity degree of 1% means that disturbations of seismic wave propagation velocity in the subsurface layer reach 1%.

3. Discussion and results

The analysis made in this paper shows that the averaged maximum velocity of ground vibration decreases with the change of seismic source, for either model: with a homogeneous subsurface layer and inhomogeneous layer. For each location of the tremor hypocenter the velocities are larger for a model with inhomogeneous subsurface layer. The effect of inhomogeneity on average maximum velocity is greater for a model with faults than it is for a monoclinal model.

The distribution of maximum ground vibration velocities depends on a depth to the seismic wave source and is most diverse for shallowest sources. Inhomogeneities occurring in the subsurface layer cause a slight reduction of values of ground vibration velocity. Small changes in the average maximum velocities and maximum ground vibrations are mainly related to small thickness of the subsurface layer, which is much smaller than the thickness of all other geological layers in the model.

Changing the angle of inclination of the fault plane, for the assumed shearing mechanism, causes that maximum ground vibration velocities do not coincide with the tremor epicenter. The symmetry of the plot of maximum velocity changes, observed for the same values but different signs of the inclination angle of nodal planes, proves that the source mechanism has more effects on the location of maximum vibrations than inhomogeneous subsurface layer has.

A linear dependence between the inhomogeneity degree and average maximum ground vibration velocity was observed. A subtle influence of the inhomogeneity on vibration velocity values is related to small size of the overburden layer.

The basic limitation of the presented approach is significant requirement for calculation facilities. The application of the staggered-grid finite-difference method into numerical solution of equation of motion needs a computational environment with high power and large memory reserves. Those requirements constrict possible users of the presented method.

The study was financed from the statutory research project No 11.11.140.561 of the Department of Geoinformatics and Applied Computer Science, AGH UST.

REFERENCES

Danek T., Franczyk A., 2004 – Parallel and distributed seismic wave field modeling. Task Quarterly 8, No 4, 573–581.

Danek T., Pięta A., Leśniak A., 2008 – Simulation of seismic waveforms from "Rudna" copper mine, Poland, using staggered grid. 31st General assembly of the European Seismological Commission: Hersonissos, Kreta, Grece.

Oberc J., Serkies J., 1970 – Origin and development of Lubin Copper Deposits. Publication of Wroclaw Scientific Society, B Series no 160, Wroclaw (in polish).

Pięta A., Danek T., Leśniak A., 2009 – Full waveform modeling of earthquakes induced by mining activities at Rudna Copper Mine. General Assembly of International Association of Seismology and Physics of the Earth's Interior (IASPEI 2009) Cape Town, Republic of South Africa.

Plewa S., 1977 – Results of petrophysical analysis of rock parameters. Geological Archives, Polish Science Academy, Cracow. Commission of Geological Sciences, Wroclaw (in polish).

Virieux J., 1986 – P-SV wave propagation in heterogeneous media: Velocity-stress finite-difference method. Geophysics, 51–4, 889–901.

NUMERICAL MODELING OF GROUND VIBRATION CAUSED BY UNDERGROUND TREMORS IN THE LGOM MINING AREA

Key words

Modeling of ground vibration, staggered grid method, seismic wave propagation

Abstract

The paper presents estimation of ground vibration by means of full wave field modeling. A geological model from the Rudna copper mine was employed, and an inhomogeneous subsurface layer was added to it.

A staggered-grid finite-difference method was applied to numerical solution of the wave equation. As compared to the traditional finite-difference approach, this method ensures better stability of solutions for high wave frequencies at a given spatial sampling step. Because of a significant amount of modeling and very large size of the model and small sampling step both in time and space, a lot of time-consuming numerical calculations were carried out. The so complicated computational problem exacted that the calculations were made in parallel on an effective computer cluster.

At the initial stage, modeling was performed with the use of a source mechanism in the form of double couple force consistent with the local orientation of tectonic stress. The local orientation was determined based on analysis of archive strong tremors recorded over the study area. At the next stages of the modeling, the orientation of nodal planes was changed all about that direction. As a result, effects of orientation of source forces on the magnitude of recorded ground vibrations could be studied. It was assumed that seismic sources were located at different depths in a dolomite layer. The ground vibration modeling was also carried out for variable depth of seismic wave source for two regions with different tectonic structure. Furthermore, the inhomogeneity degree of the subsurface layer was also changed in the modeling.

The proposed method allows maximum vibration velocities to be estimated at each site at the surface of the study area; furthermore it enables the estimation of ground vibration at sites where seismic sensors were not installed. The method can be useful for precise evaluation of effects of mining-induced seismic tremors.

MODELOWANIE NUMERYCZNE DRGAŃ POWIERZCHNI TERENU WYWOŁANYCH WSTRZĄSEM SEJSMICZNYM DLA WYBRANYCH WARUNKÓW GEOLOGICZNYCH LGOM

Słowa kluczowe

Modelowanie drgań cząstek gruntu, metoda siatek przesuniętych, propagacja fali sejsmicznej

Streszczenie

W artykule przeprowadzono estymację wielkości drgań cząstek górotworu używając modelowania pełnego pola falowego. Używano modelu ośrodka geologicznego z rejonu kopalni miedzi „Rudna" z wprowadzoną przypowierzchniową warstwą niejednorodną.

Do numerycznego rozwiązania równania falowego wykorzystano metodę różnic skończonych w odmianie tzw. przesuniętych siatek. Metoda ta w stosunku do tradycyjnej metody różnic skończonych pozwala na uzyskanie dla wysokich częstotliwości fali większej stabilności rozwiązań przy określonym przestrzennym kroku próbkowania. Duża liczba modelowań oraz bardzo duże wymiary modelu i mały krok próbkowania zarówno w czasie jak i w przestrzeni wymagały przeprowadzenia bardzo dużej liczby czasochłonnych obliczeń numerycznych. Tak duża złożoność problemu obliczeniowego wymusiła prowadzenie obliczeń w wariancie równoległym na wydajnym klastrze komputerowym.

Na etapie wstępnym modelowania były prowadzone z użyciem mechanizmu źródła w postaci podwójnej pary sił, zgodnej z lokalną orientacją naprężeń tektonicznych. Orientacja ta została ustalona na podstawie analizy dużych wstrząsów archiwalnych zarejestrowanych w tym rejonie. W kolejnych etapach modelowania zmieniano orientację płaszczyzn modalnych wokół tego kierunku. Umożliwiło to analizę wpływu orientacji sił działających w źródle na wielkość rejestrowanych drgań. Modelowania były prowadzone przy założeniu, że źródła wstrząsów są zlokalizowane na różnych głębokościach w warstwie dolomitów. Przeprowadzono również modelowania drgań dla zmiennej głębokości źródła fali sejsmicznej dla dwóch rejonów o odmiennej budowie tektonicznej. Modelowania były ponadto prowadzone przy zmieniającym się stopniu niejednorodności w warstwie przypowierzchniowej.

Opracowana metodyka pozwala na estymację maksymalnych prędkości drgań we wszystkich miejscach na powierzchni terenu a także umożliwia estymację wielkości drgań na terenach, gdzie czujniki sejsmiczne nie zostały zamontowane. Opisana metoda może być pomocna w prowadzeniu dokładnej oceny powierzchniowych skutków drgań sejsmicznych indukowanych działalnością górniczą.